



# 2D modeling of plasma-assisted H<sub>2</sub>/air ignition in a nanosecond discharge with detailed chemistry

Xingqian Mao<sup>1</sup>, Hongtao Zhong<sup>2</sup> and Yiguang Ju<sup>3</sup>  
*Princeton University, Princeton, NJ 08544, USA*

**This work studied the ignition enhancement and ignition kernel development of H<sub>2</sub>/air mixtures in a nanosecond discharge between two cylindrical electrodes at atmospheric pressure and an initial temperature of 1000 K. A two-dimensional multi-scale adaptive reduced chemistry solver for plasma assisted combustion (MARCS-PAC) with detailed combustion chemistry and transport properties was developed and validated by incorporating the plasma solver PASSKEy and the unsteady reactive flow solver ASURF+. The results show that the streamer propagates between the two electrodes and creates chemically active excited species as well as radicals together with fast gas heating. The plasma-generated active species and gas heating significantly enhance low temperature ignition. In addition, the electrode separation distance also affects the ignition kernel development. This work provides an important tool to understand kinetic enhancement of non-equilibrium plasma ignition and optimize ignitor design.**

## I. Introduction

In the past decades, non-equilibrium plasma has been applied widely in ignition enhancement, flame stabilization and fuel reforming<sup>[1, 2]</sup>. The plasma species generated by non-equilibrium excitation and fast gas heating can dramatically accelerate the low-temperature combustion chemistry<sup>[3]</sup>. Researchers have achieved promising results of plasma assisted combustion with different types of plasma discharges<sup>[4-6]</sup>. Despite these, the underlying physical-chemical mechanism between the coupling of plasma discharge and combustion process are still not well-understood.

Despite the insights into the plasma enhancement on combustion by experimental methods, different numerical models have been developed in the past years, such as the zero-dimensional (0D)<sup>[7-9]</sup>, one-dimensional (1D)<sup>[10]</sup> and two-dimensional (2D)<sup>[11, 12]</sup> numerical models. Among these models, the multi-dimensional models provide a better understanding for the interactions between plasma discharge and combustion with the incorporation of Poisson's equation for plasma discharge and reactive flow models.

Kobayashi *et al.*<sup>[13]</sup> studied the 2D nanosecond discharges between two point electrodes for H<sub>2</sub>/air mixtures. The results suggested that it would be interesting to study the effects of non-uniform distributions of radical densities and gas temperature generated by plasma on ignition at longer timescales by using 2D reactive flow simulations. Tholin *et al.*<sup>[11]</sup> studied the thermal and chemical effects of a nanosecond spark discharge on lean H<sub>2</sub>-air flame by 2D simulations. In their work, Euler equations and reduced mechanism were used. Sharma *et al.*<sup>[12]</sup> studied the nanosecond pulsed plasma induced flame ignition and combustion for a lean H<sub>2</sub>/air mixture at high pressure by a fully coupled 2D modeling with Euler equations. Sun *et al.*<sup>[14]</sup> developed a multi-scale adaptive reduced chemistry solver (MARCS) to conduct efficient combustion modeling in multi-dimensional geometries. All these studies advanced the understanding of plasma assisted ignition by 2D numerical methods.

In this work, a two-dimensional multi-scale adaptive reduced chemistry solver for plasma assisted combustion (MARCS-PAC) with detailed combustion chemistry and transport properties is developed and validated by incorporating the plasma solver PASSKEy<sup>[15, 16]</sup> and the unsteady reactive flow solver ASURF+<sup>[17]</sup>. This solver is

<sup>1</sup> Postdoctoral Research Associate, Department of Mechanical and Aerospace Engineering, [xingqian@princeton.edu](mailto:xingqian@princeton.edu).

<sup>2</sup> Ph.D. Candidate, Department of Mechanical and Aerospace Engineering, AIAA Student Member.

<sup>3</sup> Robert Porter Patterson Professor, Department of Mechanical and Aerospace Engineering, AIAA Associate Fellow.

used to model the transient plasma assisted H<sub>2</sub>/air ignition. Firstly, the MARCS-PAC model is developed and validated by shock formation, ignition, and flame propagation respectively. Secondly, the discharge streamer formation and propagation, excited species and radical production by non-equilibrium excitation, and temperature distribution by fast gas heating between two cylindrical electrodes in a nanosecond discharge are studied. Finally, the effects of non-equilibrium excitation by plasma and gas heating on H<sub>2</sub>/air ignition kernel formation and propagation are demonstrated. Moreover, the effect of electrode separation distance on ignition kernel development is examined.

## II. Numerical methods

The 2-D MARCS-PAC solver incorporates the 2-D plasma solver PASSKEY and the unsteady, compressible and multi-component reactive flow module from ASURF+. The governing equations are described as below.

The continuity equation, Poisson's equation and plasma kinetics are solved in PASSKEY to get the time evolution and spatial distribution of species and electric field during the discharge and afterglow.

The continuity equation for the species of plasma discharge is

$$\frac{\partial n_k}{\partial t} + \vec{\nabla} \cdot \vec{J}_k = \omega_k^{\text{plasma}} \quad (1)$$

$$\omega_k^{\text{plasma}} = S_k + S_{\text{ph}} \quad (2)$$

where  $n_k$  is the number density of species  $k$ ,  $\vec{J}_k$  is the flux vector of species  $k$  (x-direction and y-direction) due to the drift-diffusion of charged species by the electric field, and  $\omega_k^{\text{plasma}}$  is the production or consumption rate of species  $k$  contributed by plasma kinetics  $S_k$  and photoionization  $S_{\text{ph}}$ . As the photoionization model of H<sub>2</sub>/O<sub>2</sub>/N<sub>2</sub> mixture is not available in the literature, the ionization of O<sub>2</sub> molecules by VUV-radiation coming from electronically excited N<sub>2</sub><sup>\*</sup> (in the wavelength range of 98-102.5 nm) is considered [18]. The photoionization source term is calculated by the three-term Helmholtz equations [19].

The electric potential is calculated by Poisson's equation

$$\vec{\nabla} \cdot (-\epsilon_0 \epsilon \vec{\nabla} \phi) = q_e \sum_k Z_k n_k \quad (3)$$

where  $\epsilon_0$  is the permittivity of free space,  $\epsilon$  is the relative dielectric constant,  $\phi$  is the electric potential,  $q_e$  is the absolute value of electron charge, and  $Z_k$  is the charge of species  $k$  (1 for positive ions, and -1 for negative ions and electron).

The rate constants of electron impact reactions, transport parameters for electron, and the mean electron energy are pre-calculated by using BOLSIG+ [20]. The electron energy during the discharge is obtained by the local field approximation at atmospheric pressure [21].

The plasma module is coupled with the unsteady compressible Navier-Stokes (N-S) equations. The conservation equations of mass, species, momentum and energy are listed as below,

$$\frac{\partial \rho}{\partial t} + \vec{\nabla} \cdot (\rho \vec{V}) = 0 \quad (4)$$

$$\frac{\partial(\rho u)}{\partial t} + \vec{\nabla} \cdot (\rho u \vec{V}) = -\frac{\partial p}{\partial x} + \vec{\nabla} \cdot \vec{\tau} \quad (5)$$

$$\frac{\partial(\rho v)}{\partial t} + \vec{\nabla} \cdot (\rho v \vec{V}) = -\frac{\partial p}{\partial y} + \vec{\nabla} \cdot \vec{\tau} \quad (6)$$

$$\frac{\partial e}{\partial t} + \vec{\nabla} \cdot (e \vec{V}) = -p \vec{\nabla} \cdot \vec{V} - \vec{\nabla} \cdot \vec{q} + \vec{\nabla} \cdot (\vec{\tau} \vec{V}) + S_{\text{heat}} \quad (7)$$

where  $\rho$  is the gas mass density,  $t$  is the time,  $\vec{V} = (u, v)$  is the velocity vector,  $u$  is the velocity of x-axis,  $v$  is the velocity of y-axis,  $\vec{\tau}$  is the viscous stress tensor,  $e$  is the total energy per unit volume,  $p$  is the pressure, and  $\vec{q}$  is the heat flux. The gas heating  $S_{\text{heat}}$  from the plasma kinetics is a source term of eq.(7). The conservation equations at cylindrical coordinates are also implemented in the model.

The conservation of species  $k$  is given by the species-mass-balance equations

$$\frac{\partial(\rho Y_k)}{\partial t} + \vec{\nabla} \cdot [\rho(\vec{V} + \vec{V}_k) Y_k] = \omega_k^{\text{combustion}} \quad (8)$$

where  $Y_k$  is the mass fraction of species  $k$ ,  $\vec{V}_k$  is the diffusion velocity vector, and  $\omega_k^{\text{combustion}}$  is the production or consumption rate of species  $k$  contributed by combustion kinetics. The diffusion velocity  $\vec{V}_k$  is obtained by the summation of ordinary diffusion velocity, thermal diffusion velocity as well as the correction velocity which insures the compatibility of species and mass conservation equations.

Despite the heat release from plasma kinetics, the coupling of plasma and reactive flow module is carried out by

$$\omega_k = \omega_k^{\text{plasma}} + \omega_k^{\text{combustion}} \quad (9)$$

where  $\omega_k$  is the production or consumption rate of species  $k$ .

A plasma assisted  $\text{H}_2/\text{O}_2/\text{N}_2$  combustion mechanism is developed in this work. The mechanism consists of both plasma and combustion sub-mechanisms. The plasma mechanism consists of the reactions of electronically excited species  $\text{N}_2(\text{A})$  (summation of  $\text{N}_2(\text{A}^3\Sigma_u^+, v=0-4)$ ,  $\text{N}_2(\text{A}^3\Sigma_u^+, v=5-9)$  and  $\text{N}_2(\text{A}^3\Sigma_u^+, v=10-)$ ),  $\text{N}_2(\text{B})$  (summation of  $\text{N}_2(\text{B}^3\Pi_g)$ ,  $\text{N}_2(\text{W}^3\Delta_u)$  and  $\text{N}_2(\text{B}^3\Sigma_u^-)$ ),  $\text{N}_2(\text{a}')$  (summation of  $\text{N}_2(\text{a}^1\Sigma_u^-)$ ,  $\text{N}_2(\text{a}^1\Pi_g)$  and  $\text{N}_2(\text{w}^1\Delta_u)$ ),  $\text{N}_2(\text{C})$  (summation of  $\text{N}_2(\text{C}^3\Pi_u)$ ,  $\text{N}_2(\text{E}^3\Sigma_g^+)$  and  $\text{N}_2(\text{a}''^1\Sigma_g^+)$ ),  $\text{O}(\text{D})$  and  $\text{N}(\text{D})$ ; ions  $\text{H}_2^+$ ,  $\text{O}_2^+$ ,  $\text{N}_2^+$ ,  $\text{N}_4^+$ ,  $\text{O}^-$  and  $\text{O}_2^-$ ; and electrons. For the combustion mechanism, a detailed  $\text{H}_2/\text{O}_2/\text{N}_2$  combustion mechanism from HP-Mech [22] with  $\text{NO}_x$  formation mechanism [23, 24] are used. The mechanism consists of 29 species, 49 reactions in plasma mechanism and 73 reactions in combustion mechanism.

### III. Results and discussion

To validate the performance of present model on flame propagation, the laminar flame speed is simulated and compared with the results for PREMIX [25] which is widely used in the study of planar flames. The mixture used is a stoichiometric  $\text{H}_2/\text{air}$  mixture ( $0.296 \text{ H}_2/0.148 \text{ O}_2/0.556 \text{ N}_2$ ) with pressure of 1 atm and temperature of 298 K. Fig. 1 shows the comparison of temperature distribution of the  $\text{H}_2/\text{air}$  planar flame calculated by PREMIX and present model. The temperature distribution agrees well with the results from the PREMIX. The difference of predicted flame speed is within 5%. This indicates the accuracy of present model in predicting the flame propagation.

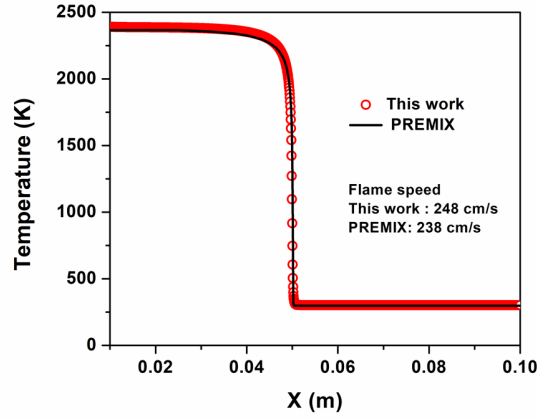


**Fig. 1 Comparison of the temperature distribution for a stoichiometric  $\text{H}_2/\text{air}$  planar flame at 298 K and 1atm between this work and PREMIX.**

For the study of plasma assisted  $\text{H}_2/\text{O}_2/\text{N}_2$  ignition, a nanosecond discharge with a single pulse is applied to the cylindrical electrodes. The length of the electrodes is 5 mm and the diameter is 2 mm. The gap distance between anode and cathode is 2 mm. The applied voltage pulse is 6.5 ns with a peak voltage of 5 kV. The geometry of the electrodes and the applied voltage are shown in Fig. 2.

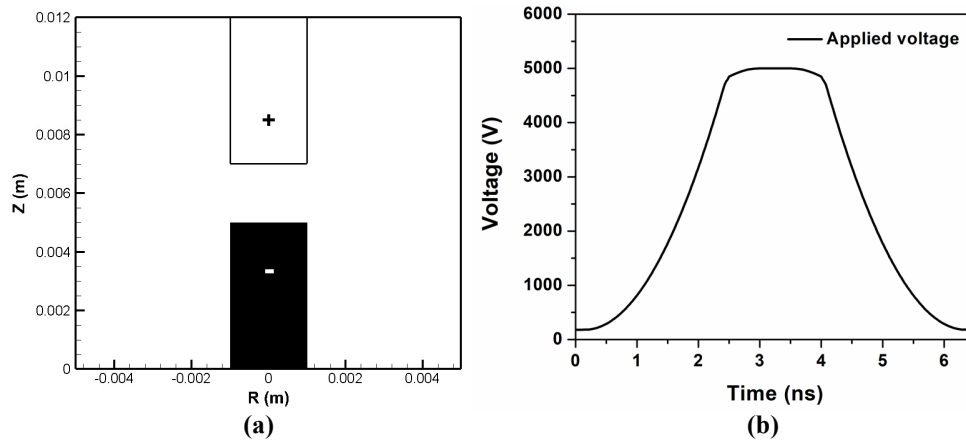


**Fig. 2 (a) Electrodes geometry and (b) applied voltage.**

In this work, the axisymmetric streamers propagation between two cylindrical electrodes are studied. Therefore, the cylindrical coordinates ( $Z, R$ ) are used for the numerical modeling, where  $Z$ -axis is the axis of discharge and  $R$ -axis is the direction of electrode diameter. To reduce the computational cost, half of the electrodes geometry is solved. The total computational domain is  $5 \text{ mm} \times 12 \text{ mm}$ , which is  $[0 \text{ mm}; 5 \text{ mm}]$  in  $R$ -axis and  $[0 \text{ mm}; 12 \text{ mm}]$  in  $Z$ -axis as shown in Fig. 2(a). A fine and uniform square mesh is used in the streamer propagation region with the mesh size of  $10 \mu\text{m} \times 10 \mu\text{m}$ , and the mesh size increases exponentially up to the rest of the computational domain.

The modeling is conducted in a stoichiometric  $\text{H}_2/\text{air}$  mixture ( $0.296 \text{ H}_2/0.148 \text{ O}_2/0.556 \text{ N}_2$ ) with initial pressure of 1 atm and temperature of 1000 K. The time evolution of electron number density during the discharge is shown in Fig. 3. Fig. 3 shows the propagation and connection of positive and negative streamer discharges during the voltage pulse. It is observed that the initial streamer forms at the tips of the electrodes due to the maximum curvature. At 3 ns, the electron distribution is more diffuse and the streamer propagates faster at the cathode than the anode before the connection. The connection between the anode and cathode occurs at around 4 ns. After 4 ns, the electron density increases dramatically in the streamer and the energy is deposited rapidly into the plasma.

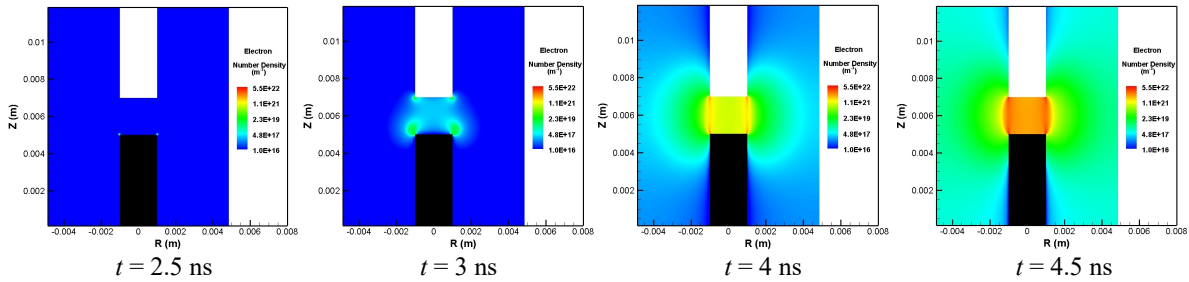


Fig. 3 Time evolution of electron number density during the discharge.

Due to the non-equilibrium excitation effects of plasma, excited species and radicals are generated during the discharge. In the afterglow, the quenching of excited species provides gas heating and radical production, such as electronically excited  $\text{N}_2(\text{A}, \text{B}, \text{a}', \text{C})$ . This accelerates the combustion reactions and enhances ignition dramatically. Fig. 4 shows the time evolution of  $\text{O}(\text{D})$  mole fraction, which is one of the key excited species generated in the  $\text{H}_2/\text{air}$  plasma. It is observed that the mole fraction of  $\text{O}(\text{D})$  increases in the streamer due to the electron impact dissociation reaction  $\text{e} + \text{O}_2 \rightarrow \text{e} + \text{O} + \text{O}(\text{D})$ . After the discharge,  $\text{O}(\text{D})$  is mainly consumed by  $\text{O}(\text{D}) + \text{H}_2 \rightarrow \text{OH} + \text{H}$  and also quenched by  $\text{O}(\text{D}) + \text{O}_2/\text{N}_2 \rightarrow \text{O} + \text{O}_2/\text{N}_2$ . This enhances the following ignition and ignition kernel propagation by providing OH and H radicals as well as gas heating.

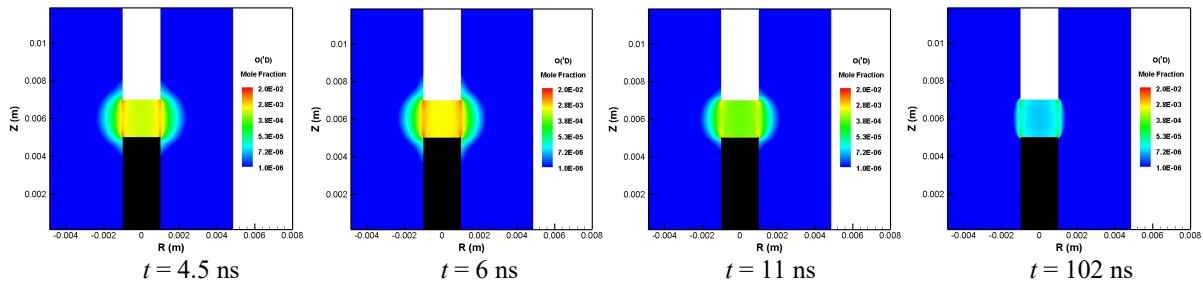
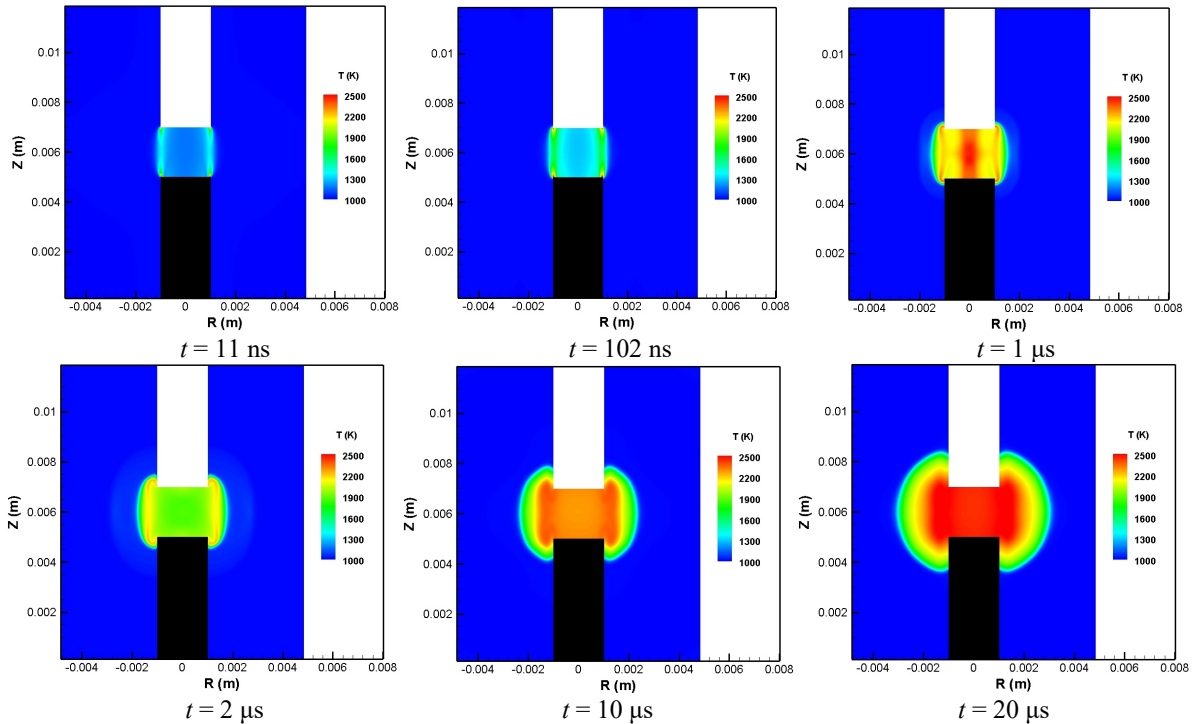


Fig. 4 Time evolution of  $\text{O}(\text{D})$  mole fraction.

To understand the effects of plasma discharge in enhancing ignition kernel formation, development and propagation, the time evolution of temperature is shown in Fig. 5. The detailed combustion chemistry with  $\text{NO}_x$  formation is incorporated to simulate the  $\text{H}_2/\text{air}$  ignition and flame propagation. In the afterglow of discharge, due to quenching of excited species, the mixture temperature increases in the streamer at the timescale of  $\sim 100 \text{ ns}$ . The temperature rise from plasma discharge is the highest near the electrode tips, as can be seen the results at 11 ns and 102 ns. At  $0.1\text{-}1 \mu\text{s}$ , the gas heating and the radical production from discharge accelerate the initial ignition kernel development in the streamer near the electrode tips between anode and cathode. The ignition then propagates towards the inner electrodes gap and outside of the electrode. Due to higher temperature and radical concentrations in the electrodes gap, ignition kernel propagates faster in the center of the electrode gap, as shown at  $1 \mu\text{s}$  in Fig. 5. At the timescale of microseconds, the ignition kernel is formed in the discharge gap and propagates to unburned region. In addition, the separation distance between the two electrodes will affect the discharge and the ignition kernel development.



**Fig. 5 Time evolution of temperature in ignition kernel development and propagation.**

#### IV. Conclusion

A two-dimensional multi-scale adaptive reduced chemistry solver for plasma assisted combustion (MARCS-PAC) with detailed combustion chemistry and transport properties was developed and validated in this work. The solver incorporated the plasma solver PASSKEY and the unsteady reactive flow solver ASURF+. The ignition enhancement of a stoichiometric  $H_2$ /air mixture by a nanosecond discharge between two cylindrical electrodes with an initial temperature of 1000 K at atmospheric pressure is studied by using the MARCS-PAC solver. The results show that the chemically active excited species, radicals and fast gas heating are produced during the streamer propagation between the two electrodes and enhance low temperature ignition dramatically. Specifically, the quenching of excited species in the afterglow also provides gas heating and radical production, such as via reactions  $O(^1D) + H_2 \rightarrow OH + H$  and  $O(^1D) + O_2/N_2 \rightarrow O + O_2/N_2$ . The results show that the radical production and gas heating from the discharge streamer accelerate the formation and development of ignition kernel. The ignition kernel development is also affected by the electrode separation distances.

#### Acknowledgments

This work was partly supported by the grants of DOE Plasma Science Center (DE-SC0020233) and National Science Foundation (CBET-1903362 and NSF-EFRI CBET-2029425). The authors would like to thank the great help of the young research group at Atelier des Plasmas in implementing the PASSKEY solver.

#### References

- [1] Ju, Y., and Sun, W., "Plasma assisted combustion: Dynamics and chemistry," *Progress in Energy and Combustion Science*, Vol. 48, 2015, pp. 21-83.
- [2] Starikovskiy, A., and Aleksandrov, N., "Plasma-assisted ignition and combustion," *Progress in Energy and Combustion Science*, Vol. 39, 2013, pp. 61-110.
- [3] Ju, Y., Lefkowitz, J. K., Reuter, C. B., Won, S. H., Yang, X., Yang, S., Sun, W., Jiang, Z., and Chen, Q., "Plasma Assisted Low Temperature Combustion," *Plasma Chemistry and Plasma Processing*, Vol. 36, No. 1, 2016, pp. 85-105.
- [4] Zhong, H., Mao, X., Rousso, A. C., Patric, C. L., Yan, C., Xu, W., Chen, Q., Wysocki G., and Ju, Y., "Kinetic study of plasma-assisted n-dodecane/ $O_2/N_2$  pyrolysis and oxidation in a nanosecond-pulsed discharge," *Proceedings of the Combustion Institute*, 2020. <https://doi.org/10.1016/j.proci.2020.06.016>

- [5] Chintala, N., Bao, A., Lou, G., and Adamovich, I. V., "Measurements of combustion efficiency in nonequilibrium RF plasma-ignited flows," *Combustion and Flame*, Vol. 144, 2006, pp. 744–756.
- [6] Dunn, I., Ahmed, K.A., Leiweke, R.J., and Ombrello, T., "Optimization of flame kernel ignition and evolution induced by modulated nanosecond-pulsed high-frequency discharge," *Proceedings of the Combustion Institute*, 2020. <https://doi.org/10.1016/j.proci.2020.06.104>
- [7] Lefkowitz, J. K., Guo, P., Rousso, A., and Ju, Y., "Species and temperature measurements of methane oxidation in a nanosecond repetitively pulsed discharge," *Philosophical Transactions of the Royal Society A*, Vol. 373, No. 2048, 2015, 20140333.
- [8] Mao, X., Chen, Q., Rousso, A. C., Chen, T. Y., and Ju, Y., "Effects of controlled non-equilibrium excitation on H<sub>2</sub>/O<sub>2</sub>/He ignition using a hybrid repetitive nanosecond and DC discharge," *Combustion and Flame*, Vol. 206, 2019, pp. 522–535.
- [9] Mao, X., Chen, Q., and Guo, C., "Methane pyrolysis with N<sub>2</sub>/Ar/He diluents in a repetitively-pulsed nanosecond discharge: Kinetics development for plasma assisted combustion and fuel reforming," *Energy Conversion and Management*, Vol. 200, 2019, 112018.
- [10] Yang, S., Nagaraja, S., Sun, W., and Yang, V., "Multiscale modeling and general theory of non-equilibrium plasma-assisted ignition and combustion," *Journal of Physics D: Applied Physics*, Vol. 50, 2017, 433001.
- [11] Tholin, F., Lacoste, D., and Bourdon, A., "Influence of fast-heating processes and O atom production by a nanosecond spark discharge on the ignition of a lean H<sub>2</sub>-air premixed flame," *Combustion and Flame*, Vol. 161, 2014, pp. 1235-1246.
- [12] Sharma, A., Subramaniam, V., Solmaz, E., and Raja, L. L., "Fully coupled modeling of nanosecond pulsed plasma assisted combustion ignition," *Journal of Physics D: Applied Physics*, Vol. 52, 2019, 095204.
- [13] Kobayashi, S., Bonaventura, Z., Tholin, F., Popov N. A., and Bourdon, A., "Study of nanosecond discharges in H<sub>2</sub>-air mixtures at atmospheric pressure for plasma assisted combustion applications," *Plasma Sources Science and Technology*, Vol. 26, 2017, 075004.
- [14] Sun, W., "Developments of Efficient Numerical Methods for Combustion Modeling with Detailed Chemical Kinetics," Ph.D. Dissertation, The Dept. of Mechanical and Aerospace Engineering, Princeton University, Princeton, NJ, 2020.
- [15] Zhu, Y., Shcherbanev, S., Baron, B., and Starikovskaia, S., "Nanosecond surface dielectric barrier discharge in atmospheric pressure air: I. measurements and 2D modeling of morphology, propagation and hydrodynamic perturbations," *Plasma Sources Science Technology*, Vol. 26, 2017, 125004.
- [16] Zhu, Y., and Starikovskaia, S., "Fast gas heating of nanosecond pulsed surface dielectric barrier discharge: Spatial distribution and fractional contribution from kinetics," *Plasma Sources Science Technology*, Vol. 27, 2018, 124007.
- [17] Zhang, T., Sun, W., Wang, L., and Ju, Y., "Effects of low-temperature chemistry and turbulent transport on knocking formation for stratified dimethyl ether/air mixtures," *Combustion and Flame*, Vol. 200, 2019, pp. 342-353.
- [18] Pancheshnyi, S., "Photoionization produced by low-current discharges in O<sub>2</sub>, air, N<sub>2</sub> and CO<sub>2</sub>," *Plasma Sources Science and Technology*, Vol. 24, 2015, 015023.
- [19] Bourdon, A., Pasko, V. P., Liu, N. Y., C'elestin, S., S'egur, P., and Marode, E., "Efficient models for photoionization produced by non-thermal gas discharges in air based on radiative transfer and the Helmholtz equations," *Plasma Sources Science Technology*, Vol. 16, 2007, pp. 656-678.
- [20] Hagelaar, G. J. M., and Pitchford, L. C., "Solving the Boltzmann equation to obtain electron transport coefficients and rate coefficients for fluid models," *Plasma Sources Science and Technology*, Vol. 14, No. 4, 2005, pp. 722-733.
- [21] Černák, M., Hoder, T., and Bonaventura, Z., "Streamer breakdown: cathode spot formation, Trichel pulses and cathode-sheath instabilities," *Plasma Sources Science and Technology*, Vol. 29, 2020, 013001.
- [22] Yang, X., Shen, X., Santner, J., Zhao, H., and Ju Y., Princeton HP-Mech. <http://engine.princeton.edu/mechanism/HP-Mech.html>, 2017.
- [23] Zhao, H., Wu, L., Patrick, C., Zhang, Z., Rezgui, Y., Yang, X., Wysocki, G., and Ju, Y., "Studies of low temperature oxidation of n-pentane with nitric oxide addition in a jet stirred reactor," *Combustion and Flame*, Vol. 197, 2018, pp. 78–87.
- [24] Gokulakrishnan, P., Fuller, C. C., and Klassen, M. S., "Experimental and modeling study of C1–C3 hydrocarbon ignition in the presence of nitric oxide," *Journal of Engineering for Gas Turbines and Power*, Vol. 140, No. 4, 2018, 041509.
- [25] Kee, R.J., Grcar, J.F., Smooke, M.D., and Miller, J.A., "A FORTRAN program for modeling steady laminar one-dimensional premixed flames," Sandia National Laboratory Report SAND85-8240, 1985.